Eur. Phys. J. C (2019) 79:403
https://doi.org/10.1140/epjc/s10052-019-6913-2

THE EUROPEAN PHYSICAL JOURNAL C

Regular Article - Theoretical Physics

J/ψ and η_c in asymmetric hot magnetized nuclear matter: a unified approach of Chiral $SU(3)$ model and QCD sum rules

Rajesh Kumar[a], **Arvind Kumar**[b]

Department of Physics, Dr. B R Ambedkar National Institute of Technology Jalandhar, Jalandhar, Punjab 144011, India

Received: 13 December 2018 / Accepted: 3 May 2019

Abstract We investigate the mass-shift of vector channel J/ψ and pseudoscalar channel η_c in strongly magnetized asymmetric nuclear medium at finite temperature using the conjunction of chiral $SU(3)$ model with the QCD sum rules. The magnetic field dependence of scalar gluon condensate $\left\langle \frac{\alpha_s}{\pi} G^a_{\mu\nu} G^{a\mu\nu} \right\rangle$ as well as the twist-2 gluon condensate $\left\langle \frac{\alpha_s}{\pi} G^a_{\mu\sigma} G^{a}{}_{\nu}{}^{\sigma} \right\rangle$ calculated from chiral SU(3) model, are implemented in QCD sum rules to calculate the magnetic field dependence of J/ψ and η_c meson masses. The effects of constant external magnetic field at finite density and temperature of the medium are found to be appreciable in symmetric and asymmetric nuclear matter. The results of the present investigation may be helpful to understand the experimental observables arising from the Compressed Baryonic Matter produced in asymmetric non-central heavy ion collision experiments.

1 Introduction

The investigation of the properties of hadrons in hot and dense matter under the effect of strong external magnetic field is a challenging area of research in non-perturbative QCD regime and of very importance from non-central Heavy-Ion Collisions (HICs) point of view which aim at understanding strong interaction physics. Due to highly asymmetric nature (different numbers of neutrons and protons) of heavy-ions, it is very imperative to include the isospin asymmetry while studying the properties of mesons in nuclear matter at finite temperature. In RHIC and LHC experiments, strongly interacting matter is produced at high temperature and very low baryon density. In addition, in non-central HICs, huge magnetic fields are believed to be produced and are estimated to be of the order of $eB \sim 15m_\pi^2$ (5×10^{19} gauss) at Large Hadron Collider (LHC) CERN [$eB \sim 2m_\pi^2$ (6.5×10^{18} gauss) at Relativistic Heavy Ion Collider (RHIC) BNL] [1–3] and it decrease rapidly after the collision as the residuals move away from the collision zone. But the interaction with remnant matter leads to the generation of induced circular currents, according to Lenz's rule, which further produce the induced magnetic field along the direction of external magnetic field. These currents affect the electric conductivity of the medium, which slows down the relaxation time, hence decay rate of external magnetic field [4–10]. The above effect is known as chiral magnetic effect [2,11–13]. The external magnetic field modifies the QCD vacuum properties such as gluon condensates [14,15] and quark condensates [16–21] and due to this effect the interaction of heavy quarkonia [9,10,22,23] with strong magnetic field leads to the modification of measurable observables [7,10,24]. In Ref. [25], it is shown that the electrical conductivity of the medium is large even at temperature near T_c. The time evolution of magnetic field is a debatable topic and to have a proper estimate of relaxation time, further investigation in the solutions of magnetohydrodynamics equations are required. With the construction of CBM experimental Facility for Antiproton and Ion Research (FAIR) and Nuclotron-based Ion Collider Facility (NICA) at Dubna, Russia, we expect significant progress to understand the in-medium modifications of hadrons at high baryonic density and moderate temperature.

Strong magnetic fields also exist in the astrophysical compact objects namely magnetars. Magnetars are the neutron stars having very strong magnetic field [26,27]. It is suggested that the soft gamma-ray repeaters (SGRs) and anomalous X-ray pulsars (AXPs) reside in the category of magnetars [28,29]. The magnetic field at the interior and exterior of magnetars are believed to be as large as $\sim 10^{18}$ gauss and $\sim 10^{14}$ gauss [30], respectively. The huge magnetic field in the centre is suggested to be due to the dense quark matter magnetic core [31,32] and has been studied substantially in literature [33–37]. Also, note that the magnetic field pro-

[a] e-mail: rajesh.sism@gmail.com

[b] e-mails: iitd.arvind@gmail.com; kumara@nitj.ac.in

Published online: 14 May 2019

duced in the heavy-ion collisions is much above the field produced in magnetars and is comparable to QCD scale and hence, will play an important role in understanding the QCD phase diagram. Such strong magnetic field leads to many interesting physical phenomenon, for example, chiral separation effect [11,38–40], heavy quark transport phenomenon [41], magnetic catalysis of chiral symmetry breaking [11], inverse magnetic catalysis [11], medium modification of heavy flavoured mesons [9,10,23], magnetic inhibition at finite temperature and density [42].

Lattice QCD is the theoretical approach to study the hadron properties, and it is formulated on grid points of space and time [43]. This is applicable in the regime of low densities and high temperature, hence relevant for Relativistic Heavy Ion Collider (RHIC) and Large Hadron Collider (LHC) experiments. This framework has explained the quenched QCD properties at finite isospin density and temperature [44–46]. However, it is not applicable at high baryonic density due to sign problem [47–49]. In addition to this, different theoretical models have been built to understand the properties of hadrons in the non-perturbative regime. For finite baryonic density and temperature, these phenomenological models based on basic QCD properties, for example, chiral symmetry, confinement properties, broken scale invariance, and trace anomaly properties are constructed. Walecka model [50], Nambu–Jona–Lasinio (NJL) model [51], the Polyakov loop extended (PNJL) model [52–54], Chiral $SU(3)$ model [55–59], Coupled Channel approach [60–63], Quark Meson Coupling (QMC) model [64–69], Polyakov Quark Meson (PQM) model [70,71], QCD sum rules [72–74] are among the various approaches which are used to explore the properties of mesons at finite density and temperature.

In the present paper, we will study the properties of ground state S-wave charmonium, J/ψ and η_c, at finite density and temperature under strong external magnetic field using QCD sum rules and chiral $SU(3)$ model. QCD sum rules are used to evaluate hadronic properties, such as mass in term of condensates to get valuable information about the structure of QCD regime [72,75,76]. The mass modifications of heavy quarkonia, notably charmonium, and bottomonium have been investigated using QCD sum rules [10,22,58,77–81]. This model remarkably predicted the mass of η_c in mixed states [82]. Also, within QCD sum rules, the in-medium mass and decay width of open charm mesons have been calculated [83]. The chiral $SU(3)$ model has been used vastly to study the nuclear matter [58], kaons and antikaons in nuclear and hyperonic matter [84], finite nuclei [55] and in-medium properties of vector mesons [84,85]. This model is also generalized to $SU(4)$ to investigate the in-medium properties of D mesons [56–59]. To study the in-medium mass of J/ψ and η_c mesons, we consider the contributions of the scalar gluon condensates, $\langle \frac{\alpha_s}{\pi} G^a_{\mu\nu} G^{a\mu\nu} \rangle$ and twist-2 tensorial gluon operator, $\langle \frac{\alpha_s}{\pi} G^a_{\mu\sigma} G^{a}{}_{\nu}{}^{\sigma} \rangle$ up to dimension four [76]. The scalar gluon condensate as well as the twist-2 gluon operator in the asymmetric nuclear medium under the effect of finite magnetic field are calculated from chiral $SU(3)$ model [55] as will be discussed in detail in the next section. In this article, we use mean field approximation, which is a non-perturbative relativistic approach to solve approximately the nuclear many-body problem. In this approximation, all the meson fields are considered as classical fields, hence only the vector and scalar fields contribute to nucleon–meson interaction Lagrangian term, as expectation value of the other mesons is zero [56]. The quantum and thermal fluctuations near chiral phase transition (beyond mean field approximation) has also been studied in literature by using the Functioal Renoramalization Group (FRG) approach [86,87] and Polyakov extended quark meson (PQM) model [88,89]. It was observed that the critical point moves towards the higher chemical potential and lower temperature region [90,91]. The phase diagram become more stabilized after the inclusion of fluctuations [87].

Interest in the in-medium properties of charmonium was ignited when Matsui and Satz proposed that the decrease in the yield of J/ψ state in HICs due to color screening effect should be considered as a probe of the production of Quark Gluon Plasma (QGP) [92]. Imperative results in favor of J/ψ suppression were observed at CERN SPS and RHIC experiment [93–95]. The statistical recombination of primordially produced charm quark pairs may lead to the increase in the yield of J/ψ mesons and this picture is more important at LHC energies [96–98]. Charmonium is a bound state of charm and an anti-charm quark. The in-medium properties of charmonia are modified in the nuclear matter through gluon condensates [58,99]. The gluon condensates modify feebly, hence the obtained mass-shift of lowest charmonium states, J/ψ and η_c is very small in nuclear medium [77]. In Ref. [99], the in-medium mass of charmonium states have been studied under linear density approximation in the nuclear medium using QCD second order stark effect. A significant mass shift is observed for the excited charmonium states ($\psi(3686)$ and $\psi(3770)$), but a small mass shift for the ground state $J/\psi(3097)$. In Ref. [78], mass shift of J/ψ and η_c is studied using QCD sum rules through the medium modifications of gluon condensates in linear density approximation. These studies are applicable up to nuclear saturation density only. In Refs. [58,59], gluon condensates evaluated in non-linear chiral $SU(3)$ model, in terms of dilaton field, were used as input in QCD second order stark effect and in QCD sum rules, respectively, to evaluate the masses of charmonium at finite density and temperature. In Refs. [100–102], the effect of temperature on the J/ψ and η_c was also studied in deconfined phase and observed that the heavy quark bound states can survive in the deconfined plasma. In addition to this, the in-medium properties of excited charmonium states, χ_{c0}

and χ_{c1} are also studied in the literature [78,103]. Recently, in Ref. [10], authors have investigated the masses of lowest charmonium states J/ψ and η_c in strong magnetic field using QCD sum rules. In Ref. [22], magnetically induced mixing between J/ψ and η_c have been calculated. Also, chiral $SU(3)$ model along with QCD second order stark effect was extended in Ref. [104] to study the effect of external magnetic field on the masses of J/ψ, $\psi(3686)$ and $\psi(3770)$ mesons at finite density and zero temperature. D, B, and ρ mesons are also studied in the presence of strong magnetic field [9,23,105,106]. Due to the attractive potential of J/ψ and η_c, it is also predicted that these mesons can form a bound state with nucleons [107,108].

We organize the paper as follows. In Sect. 2, we will present chiral $SU(3)$ model to describe the hot asymmetric nuclear matter in the presence of an external magnetic field. The scalar density as well as the number density of the charged proton has contributions from the Landau energy levels, whereas, the uncharged neutrons do not have contributions from Landau energy levels. In Sect. 3, we describe the QCD sum rules to calculate the in-medium mass-shift of charmonium. We discuss the results of the present investigation in Sect. 4, and finally in Sect. 5 summary of this work will be given.

2 The hadronic chiral $SU_L(3) \times SU_R(3)$ model

We use an effective field theoretical approach to describe hadron–hadron interactions, based on the broken scale invariance [55,56,84] and non-linear realization of chiral symmetry [109–111] in the presence of external magnetic field at finite density and temperature. In this model, the hadron–hadron interactions are expressed in terms of the scalar fields σ, ζ, δ, χ and vector fields ω and ρ. The δ and ρ fields are introduced to incorporate the effect of isospin asymmetry in hadronic medium. Also, the dilaton field χ is proposed to express the scale symmetry breaking, leading to a non-vanishing trace of the energy–momentum tensor [55]. The Lagrangian density of this model under mean-field approximation is given as

$$\mathcal{L}_{chiral} = \mathcal{L}_{kin} + \sum_{M=S,V} \mathcal{L}_{NM} + \mathcal{L}_{vec} + \mathcal{L}_0 + \mathcal{L}_{SB}. \tag{1}$$

Individually,

$$\mathcal{L}_{NM} = -\sum_i \bar{\psi}_i \left[m_i^* + g_{\omega i}\gamma_0\omega + g_{\rho i}\gamma_0\rho \right] \psi_i, \tag{2}$$

$$\mathcal{L}_{vec} = \frac{1}{2}\left(m_\omega^2\omega^2 + m_\rho^2\rho^2\right)\frac{\chi^2}{\chi_0^2} + g_4(\omega^4 + 6\omega^2\rho^2 + \rho^4), \tag{3}$$

$$\mathcal{L}_0 = -\frac{1}{2}k_0\chi^2\left(\sigma^2+\zeta^2+\delta^2\right) + k_1\left(\sigma^2+\zeta^2+\delta^2\right)^2 + k_2\left(\frac{\sigma^4}{2}+\frac{\delta^4}{2}+3\sigma^2\delta^2+\zeta^4\right) + k_3\chi\left(\sigma^2-\delta^2\right)\zeta - k_4\chi^4 - \frac{1}{4}\chi^4\ln\frac{\chi^4}{\chi_0^4} + \frac{d}{3}\chi^4\ln\left(\left(\frac{\left(\sigma^2-\delta^2\right)\zeta}{\sigma_0^2\zeta_0}\right)\left(\frac{\chi}{\chi_0}\right)^3\right), \tag{4}$$

and

$$\mathcal{L}_{SB} = -\left(\frac{\chi}{\chi_0}\right)^2\left[m_\pi^2 f_\pi\sigma + \left(\sqrt{2}m_K^2 f_K - \frac{1}{\sqrt{2}}m_\pi^2 f_\pi\right)\zeta\right]. \tag{5}$$

In Eq. (1), $\mathcal{L}_{kin}$ represents the kinetic energy term, $\mathcal{L}_{NM}$ is the nucleon–meson interaction term, where S and V represents the spin-0 and spin-1 mesons, respectively. Here, the effective mass of nucleons is given as

$$m_i^* = -(g_{\sigma i}\sigma + g_{\zeta i}\zeta + g_{\delta i}\tau_3\delta). \tag{6}$$

In above, $g_{\sigma i}$, $g_{\zeta i}$ and $g_{\delta i}$ represent the coupling strengths of nucleons ($i = p, n$) with σ, ζ and δ fields respectively and τ_3 is the third component of isospin. The term $\mathcal{L}_{vec}$ of Eq. (1) generates the mass of vector mesons through the interactions with scalar mesons and contains the quartic self-interaction terms, $\mathcal{L}_0$ describes the spontaneous chiral symmetry breaking, and $\mathcal{L}_{SB}$ describes the explicit chiral symmetry breaking.

In grand canonical ensemble, the partition function for nuclear system is given by [112]

$$\mathcal{Z} = \mathrm{Tr}\exp[-\beta(\hat{\mathcal{H}} - \sum_{i=p,n}\mu_i\hat{\mathcal{N}}_i)], \tag{7}$$

where $\beta = 1/T$ and $\hat{\mathcal{H}}$, μ_i and $\hat{\mathcal{N}}_i$ are the Hamiltonian density operator, chemical potential and number density operator, respectively. The thermodynamical potential, Ω at given temperature T reads

$$\Omega(T, V, \mu) = -T\ln\mathcal{Z}. \tag{8}$$

By inserting mean field Hamiltonian density [112] in terms of Lagrangian density, the thermodynamic potential Ω, per unit volume, V in zero magnetic field can be expressed as

$$\frac{\Omega}{V} = -\frac{\gamma_i T}{(2\pi)^3}\sum_{i=p,n}\int d^3k\left\{\ln\left(1+e^{-\beta[E_i^*(k)-\mu_i^*]}\right) + \ln\left(1+e^{-\beta[E_i^*(k)+\mu_i^*]}\right)\right\} - \mathcal{L}_{vec} - \mathcal{L}_0 - \mathcal{L}_{SB} - \mathcal{V}_{vac}, \tag{9}$$

where the sum runs over neutron and proton, γ_i is the spin degeneracy factor for nucleons, $E_i^*(k) = \sqrt{k^2 + m_i^*}$ and $\mu_i^* = \mu_i - g_{\omega i}\omega - g_{\rho i}\tau_3\rho$ are the effective single particle

energy of nucleons and effective nucleon chemical potential, respectively. In addition, vacuum potential energy, $\mathcal{V}_{vac}$ is subtracted in order to get zero vacuum energy.

In the presence of magnetic field, the Lagrangian density given by Eq. (1) modifies to

$$\mathcal{L}_T = \mathcal{L}_{chiral} + \mathcal{L}_{mag}, \tag{10}$$

where

$$\mathcal{L}_{mag} = -\bar{\psi}_i q_i \gamma_\mu A^\mu \psi_i - \frac{1}{4}\kappa_i \mu_N \bar{\psi}_i \sigma^{\mu\nu} F^{\mu\nu} \psi_i - \frac{1}{4} F^{\mu\nu} F_{\mu\nu}. \tag{11}$$

In above ψ_i is a wave function corresponds to the i^{th} nucleon and the second term represents the tensorial interaction with the electromagnetic field tensor, $F_{\mu\nu}$. Also, k_i and μ_N are the anomalous magnetic moment of i^{th} nucleon and nuclear magneton, given as $\mu_N = \frac{e}{2m_N}$, respectively, where m_N is the vacuum mass of the nucleon. We choose the magnetic field to be uniform and along the Z-axis, and hence the vector potential $A^\mu = (0, 0, Bx, 0)$. In the following, we discuss the interaction of charged and uncharged particles with external magnetic field.

2.1 Charged proton in magnetic field

In the presence of uniform magnetic field, due to the charged nature of proton, Lorentz force comes into picture. Hence, the transverse momenta of proton with an electric charge q_p are confined to discrete Landau levels, ν, with, $k_\perp^2 = 2\nu|q_p|B$, where $\nu \geq 0$ is an integral quantum number [113]. Thus, the volume integral converts into line integral

$$\int d^3k \rightarrow \frac{|q_p|B}{(2\pi)^2} \sum_n \int_0^\infty dk_\parallel, \tag{12}$$

where $k_\parallel$ is the momenta along the direction of magnetic field. Also, the summation represents a sum over the discrete orbital angular momentum, n of proton in the perpendicular plane. The orbital quantum number is related to ν via $\nu = n + \frac{1}{2} - \frac{q_p}{|q_p|}\frac{s}{2} = 0, 1, 2, \ldots$. Here, the quantum number s is $+1$ for spin up and -1 for spin down protons. In addition to this, the effective single particle proton energy also gets quantized [114] and is given by

$$\tilde{E}^p_{\nu,s} = \sqrt{\left(k_\parallel^p\right)^2 + \left(\sqrt{m_p^{*2} + 2\nu|q_p|B} - s\mu_N\kappa_p B\right)^2}. \tag{13}$$

Under these changes, the first term of Eq. (9), for proton will be

$$\frac{\Omega_p}{V} = -\frac{T|q_p|B}{(2\pi)^2}\Bigg[\sum_{\nu=0}^{\nu_{max}^{(s=1)}} \int_0^\infty dk_\parallel \left\{\ln\left(1 + e^{-\beta[\tilde{E}^p_{\nu,s} - \mu_p^*]}\right) + \ln\left(1 + e^{-\beta[\tilde{E}^p_{\nu,s} + \mu_p^*]}\right)\right\} + \sum_{\nu=1}^{\nu_{max}^{(s=-1)}} \int_0^\infty dk_\parallel \left\{\ln\left(1 + e^{-\beta[\tilde{E}^p_{\nu,s} - \mu_p^*]}\right) + \ln\left(1 + e^{-\beta[\tilde{E}^p_{\nu,s} + \mu_p^*]}\right)\right\}\Bigg]. \tag{14}$$

2.2 Uncharged neutron in magnetic field

For uncharged neutron, there is no Landau quantization in the presence of external magnetic field, hence $\int \frac{d^3k}{(2\pi)^3}$ remains unchanged [113]. The first term of thermodynamic potential, Ω, per unit volume given by Eq. (9), for neutron, will be

$$\frac{\Omega_n}{V} = -\frac{T}{(2\pi)^3}\sum_{s=\pm1}\int d^3k \left\{\ln\left(1 + e^{-\beta[\tilde{E}^n_s - \mu_n^*]}\right) + \ln\left(1 + e^{-\beta[\tilde{E}^n_s + \mu_n^*]}\right)\right\}, \tag{15}$$

where $\tilde{E}^n_s$ is the effective single particle energy of neutron in the presence of magnetic field and is given by

$$\tilde{E}^n_s = \sqrt{\left(k_\parallel^n\right)^2 + \left(\sqrt{m_n^{*2} + \left(k_\perp^n\right)^2} - s\mu_N\kappa_n B\right)^2}. \tag{16}$$

The net thermodynamical potential in the presence of external magnetic field can be written as

$$\frac{\Omega}{V} = \frac{\Omega_p}{V} + \frac{\Omega_n}{V} - \mathcal{L}_{vec} - \mathcal{L}_0 - \mathcal{L}_{SB} - \mathcal{V}_{vac}. \tag{17}$$

Now, by minimizing the thermodynamical potential Ω/V of the nuclear system, the coupled equations of motion of the non-strange meson field σ, the strange scalar meson field ζ, the scalar iso-vector meson field δ, the vector meson field ω, the vector–isovector meson field ρ, and the dilaton field χ, are determined and given as

$$\begin{aligned}
\frac{\partial(\Omega/V)}{\partial\sigma} &= k_0\chi^2\sigma - 4k_1\left(\sigma^2 + \zeta^2 + \delta^2\right)\sigma \\
&\quad -2k_2\left(\sigma^3 + 3\sigma\delta^2\right) - 2k_3\chi\sigma\zeta \\
&\quad -\frac{d}{3}\chi^4\left(\frac{2\sigma}{\sigma^2 - \delta^2}\right) + \left(\frac{\chi}{\chi_0}\right)^2 m_\pi^2 f_\pi \\
&\quad -\sum g_{\sigma i}\rho_i^s = 0, \\
\frac{\partial(\Omega/V)}{\partial\zeta} &= k_0\chi^2\zeta - 4k_1\left(\sigma^2 + \zeta^2 + \delta^2\right)\zeta - 4k_2\zeta^3 \\
&\quad -k_3\chi\left(\sigma^2 - \delta^2\right)
\end{aligned} \tag{18}$$

$$-\frac{d}{3}\frac{\chi^4}{\zeta}+\left(\frac{\chi}{\chi_0}\right)^2\left[\sqrt{2}m_K^2 f_K-\frac{1}{\sqrt{2}}m_\pi^2 f_\pi\right]-\sum g_{\zeta i}\rho_i^s=0, \tag{19}$$

$$\frac{\partial(\Omega/V)}{\partial\delta}=k_0\chi^2\delta-4k_1\left(\sigma^2+\zeta^2+\delta^2\right)\delta-2k_2\left(\delta^3+3\sigma^2\delta\right)+2k_3\chi\delta\zeta+\frac{2}{3}d\chi^4\left(\frac{\delta}{\sigma^2-\delta^2}\right)-\sum g_{\delta i}\tau_3\rho_i^s=0, \tag{20}$$

$$\frac{\partial(\Omega/V)}{\partial\omega}=\left(\frac{\chi}{\chi_0}\right)^2 m_\omega^2\omega+g_4\left(4\omega^3+12\rho^2\omega\right)-\sum g_{\omega i}\rho_i^v=0, \tag{21}$$

$$\frac{\partial(\Omega/V)}{\partial\rho}=\left(\frac{\chi}{\chi_0}\right)^2 m_\rho^2\rho+g_4\left(4\rho^3+12\omega^2\rho\right)-\sum g_{\rho i}\tau_3\rho_i^v=0, \tag{22}$$

and

$$\frac{\partial(\Omega/V)}{\partial\chi}=k_0\chi\left(\sigma^2+\zeta^2+\delta^2\right)-k_3\left(\sigma^2-\delta^2\right)\zeta+\chi^3\left[1+\ln\left(\frac{\chi^4}{\chi_0^4}\right)\right]+(4k_4-d)\chi^3-\frac{4}{3}d\chi^3\ln\left(\left(\frac{\left(\sigma^2-\delta^2\right)\zeta}{\sigma_0^2\zeta_0}\right)\left(\frac{\chi}{\chi_0}\right)^3\right)+\frac{2\chi}{\chi_0^2}\left[m_\pi^2 f_\pi\sigma+\left(\sqrt{2}m_K^2 f_K-\frac{1}{\sqrt{2}}m_\pi^2 f_\pi\right)\zeta\right]-\frac{\chi}{{\chi_0}^2}(m_\omega^2\omega^2+m_\rho^2\rho^2)=0, \tag{23}$$

respectively.

In above, m_π, m_K and f_π, f_K denote the mass and decay constant of π, K mesons, respectively and the other parameters k_0, k_2 and k_4 are fitted to reproduce the vacuum mass of σ, ζ and χ meson and the remaining constants k_1 is fixed to produce the effective nucleon mass at saturation density around $0.65m_N$ and k_3 is the constraint by η and η' masses. Furthermore, ρ_i^s and ρ_i^v represent the scalar and vector/number densities of ith nucleon respectively.

In the presence of the magnetic field, the vector density as well as the scalar density of proton can be extracted from Eqs. (21) to (18) and given as [33,115]

$$\rho_p^v=\frac{|q_p|B}{2\pi^2}\left[\sum_{\nu=0}^{\nu_{max}^{(s=1)}}\int_0^\infty dk_\parallel^p\left(f_{k,\nu,s}^p-\bar{f}_{k,\nu,s}^p\right)+\sum_{\nu=1}^{\nu_{max}^{(s=-1)}}\int_0^\infty dk_\parallel^p\left(f_{k,\nu,s}^p-\bar{f}_{k,\nu,s}^p\right)\right], \tag{24}$$

and

$$\rho_p^s=\frac{|q_p|Bm_p^*}{2\pi^2}\left[\sum_{\nu=0}^{\nu_{max}^{(s=1)}}\int_0^\infty\frac{dk_\parallel^p}{\sqrt{(k_\parallel^p)^2+(\bar{m}_p)^2}}\left(f_{k,\nu,s}^p+\bar{f}_{k,\nu,s}^p\right)+\sum_{\nu=1}^{\nu_{max}^{(s=-1)}}\int_0^\infty\frac{dk_\parallel^p}{\sqrt{(k_\parallel^p)^2+(\bar{m}_p)^2}}\left(f_{k,\nu,s}^p+\bar{f}_{k,\nu,s}^p\right)\right], \tag{25}$$

respectively, where $\bar{m}_p$ is the effective mass under the effect of magnetic field, defined as

$$\bar{m}_p=\sqrt{m_p^{*2}+2\nu|q_p|B}-s\mu_N\kappa_p B. \tag{26}$$

Similarly, for the uncharged neutron, the number and scalar densities are given by [33,115]

$$\rho_n^v=\frac{1}{2\pi^2}\sum_{s=\pm1}\int_0^\infty k_\perp^n dk_\perp^n\int_0^\infty dk_\parallel^n\left(f_{k,s}^n-\bar{f}_{k,s}^n\right), \tag{27}$$

and

$$\rho_n^s=\frac{1}{2\pi^2}\sum_{s=\pm1}\int_0^\infty k_\perp^n dk_\perp^n\left(1-\frac{s\mu_N\kappa_n B}{\sqrt{m_n^{*2}+\left(k_\perp^n\right)^2}}\right)\times\int_0^\infty dk_\parallel^n\frac{m_n^*}{\tilde{E}_s^n}\left(f_{k,s}^n+\bar{f}_{k,s}^n\right), \tag{28}$$

respectively. In above, $f_{k,\nu,s}^p$, $\bar{f}_{k,\nu,s}^p$, $f_{k,s}^n$ and $\bar{f}_{k,s}^n$ represent the finite temperature distribution functions for particles and antiparticles for proton and neutron, and given as

$$f_{k,\nu,s}^p=\frac{1}{1+\exp\left[\beta(\tilde{E}_{\nu,s}^p-\mu_p^*)\right]},\qquad \bar{f}_{k,\nu,s}^p=\frac{1}{1+\exp\left[\beta(\tilde{E}_{\nu,s}^p+\mu_p^*)\right]}, \tag{29}$$

$$f_{k,s}^n=\frac{1}{1+\exp\left[\beta(\tilde{E}_s^n-\mu_n^*)\right]},\qquad \bar{f}_{k,s}^n=\frac{1}{1+\exp\left[\beta(\tilde{E}_s^n+\mu_n^*)\right]}. \tag{30}$$

If we neglect the effect of magnetic field in Eq. (10), the vector and scalar densities of the nucleons are modified and given as

$$\rho_i^v=\gamma_i\int\frac{d^3k}{(2\pi)^3}\left(\frac{1}{1+\exp\left[\beta(E_i^*(k)-\mu_i^*)\right]}-\frac{1}{1+\exp\left[\beta(E_i^*(k)+\mu_i^*)\right]}\right), \tag{31}$$

and

$$\rho_i^s = \gamma_i \int \frac{d^3k}{(2\pi)^3}\frac{m_i^*}{E_i^*(k)}\Bigg(\frac{1}{1+\exp\left[\beta(E_i^*(k)-\mu_i^*)\right]} + \frac{1}{1+\exp\left[\beta(E_i^*(k)+\mu_i^*)\right]}\Bigg), \tag{32}$$

respectively.

As discussed earlier, the effect of isospin asymmetry is introduced by incorporating δ and ρ fields having dependence on the isospin asymmetry parameter, $\eta = (\rho_n^v - \rho_p^v)/2\rho_N$, which is the measure of the abundance of one isospin component over other.

In the present investigation, gluon condensates will be used to calculate the effective mass of charmonia within QCD sum rules. The scalar gluon condensate $\left\langle\frac{\alpha_s}{\pi}G^a_{\mu\nu}G^{a\mu\nu}\right\rangle$ and the twist-2 tensorial gluon operator, $\left\langle\frac{\alpha_s}{\pi}G^a_{\mu\sigma}G^{a}{}_{\nu}{}^{\sigma}\right\rangle$, given by Eqs. (39) and (40) respectively in the following are derived in terms of medium modified σ, ζ, δ and dilaton field χ within chiral $SU(3)$ model as explained below.

Within this model, gluon condensates are obtained from the energy–momentum tensor in terms of χ field [58]. We start with energy–momentum tensor

$$T_{\mu\nu} = (\partial_\mu\chi)\left(\frac{\partial\mathcal{L}_\chi}{\partial(\partial^\nu\chi)}\right) - g_{\mu\nu}\mathcal{L}_\chi, \tag{33}$$

where $\mathcal{L}_\chi$ represents the Lagrangian density term, which is written in the model to incorporate scale breaking property of QCD and is given by

$$\mathcal{L}_\chi = \frac{1}{2}(\partial_\mu\chi)(\partial^\mu\chi) - k_4\chi^4 - \frac{1}{4}\chi^4\ln\left(\frac{\chi^4}{\chi_0^4}\right) + \frac{d}{3}\chi^4\ln\left(\left(\frac{(\sigma^2-\delta^2)\,\zeta}{\sigma_0^2\zeta_0}\right)\left(\frac{\chi}{\chi_0}\right)^3\right). \tag{34}$$

To obtain the trace of above energy–momentum tensor, we multiply it by $g^{\mu\nu}$,

$$T^\mu_\mu = (\partial_\mu\chi)\left(\frac{\partial\mathcal{L}_\chi}{\partial(\partial_\mu\chi)}\right) - 4\mathcal{L}_\chi = -(1-d)\chi^4. \tag{35}$$

The energy–momentum tensor, $T_{\mu\nu}$ and its trace, T^μ_μ in massless QCD can be written as [116,117]

$$T_{\mu\nu} = -\left(\frac{\pi}{\alpha_s}\right)\left(u_\mu u_\nu - \frac{g_{\mu\nu}}{4}\right)G_2 + \frac{g_{\mu\nu}}{4}\frac{\beta_{QCD}}{2g}G^a{}_{\sigma\kappa}G^{a\sigma\kappa}, \tag{36}$$

and

$$T^\mu_\mu = \left\langle\frac{\beta_{QCD}}{2g}G^a{}_{\sigma\kappa}G^{a\sigma\kappa}\right\rangle, \tag{37}$$

respectively. In Eq. (36), G_2 is twist-2 gluon operator.

By comparing Eq. (35) with (37), scalar gluon condensate, G_0 can be written as

$$G_0 = \left\langle\frac{\alpha_s}{\pi}G^a{}_{\mu\nu}G^{a\mu\nu}\right\rangle = \frac{8}{9}\Big[(1-d)\chi^4\Big]. \tag{38}$$

If we take the effect of finite quark mass term [58], the modified scalar gluon condensate, G_0 is expressed as

$$G_0 = \left\langle\frac{\alpha_s}{\pi}G^a{}_{\mu\nu}G^{a\mu\nu}\right\rangle = \frac{8}{9}\Bigg[(1-d)\chi^4 + \left(\frac{\chi}{\chi_0}\right)^2\Big(m_\pi^2 f_\pi\sigma + \big(\sqrt{2}m_k^2 f_k - \frac{1}{\sqrt{2}}m_\pi^2 f_\pi\big)\zeta\Big)\Bigg]. \tag{39}$$

The comparison of energy–momentum tensor in chiral model with QCD [58], gives the expression for twist-2 gluon operator and is given by

$$G_2 = \left\langle\frac{\alpha_s}{\pi}G^a_{\mu\sigma}G^{a}{}_{\nu}{}^{\sigma}\right\rangle = \frac{\alpha_s}{\pi}\Bigg[-(1-d+4k_4)(\chi^4-{\chi_0}^4) - \chi^4\ln\left(\frac{\chi^4}{{\chi_0}^4}\right) + \frac{4}{3}d\chi^4\ln\left(\left(\frac{(\sigma^2-\delta^2)\,\zeta}{\sigma_0^2\zeta_0}\right)\left(\frac{\chi}{\chi_0}\right)^3\right)\Bigg]. \tag{40}$$

The value of d may be taken from QCD beta function, β_{QCD} at the one loop level [55], with N_c colors and N_f flavors,

$$\beta_{QCD} = -\frac{11N_cg^3}{48\pi^2}\left(1-\frac{2N_f}{11N_c}\right) + \mathcal{O}(g^5). \tag{41}$$

Here, the first term in parentheses arises from the self-interaction of the gluons and the second term is proportional to N_f, is the contribution from quark pairs. This equation suggests the value $d = 6/33$ for three flavors and three colors.

3 In-medium masses of J/ψ and η_c meson in external magnetic field

In the present investigation, to study the effective mass of charmonium, we use QCD sum rules, which is a non-perturbative mechanism to study the confining nature of QCD [72,75,77]. In this approach, effective mass of mesons is obtained from the moment derived from the operator product expansion (OPE) of correlation function [72].

We start from time ordered current–current correlation function of two heavy quark currents [75].

$$\Pi^J(q) = i\int d^4x e^{iq\cdot x}\langle T[j^c(x)j^{c\dagger}(0)]\rangle. \tag{42}$$

Here, $q = (\omega, \mathbf{q})$, represents four momentum vector and symbol c stands for the pseudoscalar (P) and vector (V) mesons. Each current is defined as $j^P = \bar{\psi}_q \gamma_5 \psi_q$ and $j_\mu^V = \bar{\psi}_q \gamma_\mu \psi_q$ with ψ_q being the quark operator.

We can render the current–current correlation in the region of positive and large $Q^2 = \mathbf{q}^2 - \omega^2$ through an OPE. Hence, left-hand side of above equation can be written as [118]

$$\Pi(q) = \sum_n W_n(q) \langle \hat{O}_n \rangle. \tag{43}$$

In above, the $\hat{O}_n$ are operators of dimension n, and W_n are the perturbative Wilson coefficients.

By expressing correlation function as polarization function $\tilde{\Pi}^J$, which reduces to vacuum polarization function in the limit $\rho_N \to 0$ [77], the nth moment can be expressed as

$$\begin{aligned} M_n^J &\equiv \frac{1}{n!}\left(\frac{d}{d\omega^2}\right)^n \tilde{\Pi}^J(\omega^2)\Big|_{\omega^2=-Q_0^2}, \\ &= \frac{1}{\pi}\int_{4m_c^2}^{\infty} \frac{\mathrm{Im}\tilde{\Pi}^J(s)}{(s+Q_0^2)^{n+1}} ds, \end{aligned} \tag{44}$$

at a fixed $Q_0^2 = 4m_c^2\xi$.

Using operator product expansion, the moment M_n^J can be written as [76]

$$M_n^J(\xi) = A_n^J(\xi)\left[1 + a_n^J(\xi)\alpha_s + b_n^J(\xi)\phi_b + c_n^J(\xi)\phi_c\right], \tag{45}$$

where $A_n^J(\xi)$, $a_n^J(\xi)$, $b_n^J(\xi)$ and $c_n^J(\xi)$ are the Wilson coefficients [72,76] and ξ is the normalization scale. The common factor A_n^J results from the bare loop diagram. The coefficients a_n^J take into account perturbative radiative corrections, while the coefficients b_n^J are associated with the scalar gluon condensate through

$$\phi_b = \frac{4\pi^2}{9}\frac{\left\langle \frac{\alpha_s}{\pi} G^a_{\mu\nu} G^{a\mu\nu} \right\rangle}{(4m_c^2)^2}. \tag{46}$$

As described earlier, the contribution of the scalar gluon condensate is incorporated through the σ, ζ, δ and dilaton field χ within the chiral $SU(3)$ model. Using Eq. (39), the above equation can be rewritten in terms of these fields as

$$\begin{aligned} \phi_b = \frac{32\pi^2}{81(4m_c^2)^2}\Bigg[(1-d)\chi^4 + \left(\frac{\chi}{\chi_0}\right)^2 \Big(m_\pi^2 f_\pi \sigma \\ + \Big(\sqrt{2}m_K^2 f_K - \frac{1}{\sqrt{2}} m_\pi^2 f_\pi\Big)\zeta\Big)\Bigg]. \end{aligned} \tag{47}$$

The coefficients c_n^J are associated with the value of ϕ_c, which gives the contribution from twist-2 gluon operator, ϕ_c appearing in Eq. (45) is defined by

$$\phi_c = \frac{4\pi^2}{3(4m_c^2)^2}\left\langle \frac{\alpha_s}{\pi} G^a_{\mu\sigma} G^{a\ \sigma}_{\ \nu} \right\rangle, \tag{48}$$

where twist-2 gluon operator $\left\langle \frac{\alpha_s}{\pi} G^a_{\mu\sigma} G^{a\ \sigma}_{\ \nu} \right\rangle$ is given by Eq. (40). Explicitly in terms of σ, ζ, δ and dilaton field χ, ϕ_c will be,

$$\begin{aligned} \phi_c = \frac{4\pi^2\alpha_s}{3(4m_c^2)^2\pi}\Bigg[-(1-d+4k_4)(\chi^4 - {\chi_0}^4) - \chi^4 \ln\Big(\frac{\chi^4}{{\chi_0}^4}\Big) \\ + \frac{4}{3} d\chi^4 \ln\left(\left(\frac{(\sigma^2-\delta^2)\,\zeta}{\sigma_0^2\zeta_0}\right)\left(\frac{\chi}{\chi_0}\right)^3\right)\Bigg]. \end{aligned} \tag{49}$$

The m_c and α_s parameters are the running charm quark mass and running coupling constant and are ξ dependent [72], and are given by

$$\frac{m_c(\xi)}{m_c} = 1 - \frac{\alpha_s}{\pi}\left\{\frac{2+\xi}{1+\xi}\ln(2+\xi) - 2\ln 2\right\}, \tag{50}$$

where, $m_c \equiv m_c(p^2 = -m_c^2) = 1.26$ GeV [75], and

$$\begin{aligned} &\alpha_s\left(Q_0^2 + 4m_c^2\right) \\ &= \alpha_s\left(4m_c^2\right) \Big/ \left(1 + \frac{25}{12\pi}\alpha_s\left(4m_c^2\right)\ln\frac{Q_0^2+4m_c^2}{4m_c^2}\right), \end{aligned} \tag{51}$$

with, $\alpha_s\left(4m_c^2\right) \simeq 0.3$ and $Q_0^2 = 4m_c^2\xi$ [72].

The in-medium mass of the J/ψ and η_c charmonium states in terms of M_n^J can be written as

$$m_C^{*\,2} \simeq \frac{M_{n-1}^J(\xi)}{M_n^J(\xi)} - 4m_c^2\xi. \tag{52}$$

In the next section, we shall discuss the results for the J/ψ and η_c meson mass modifications in asymmetric nuclear matter in the presence of an external magnetic field, B, at finite temperature.

4 Results and discussions

The effects of external magnetic field in hot and dense nuclear matter on the properties of J/ψ and η_c in the present work are calculated through the in-medium behaviour of scalar gluon condensate $\left\langle \frac{\alpha_s}{\pi} G^a_{\mu\nu} G^{a\mu\nu} \right\rangle$ and the twist-2 tensorial gluon operator, $\left\langle \frac{\alpha_s}{\pi} G^a_{\mu\sigma} G^{a\ \sigma}_{\ \nu} \right\rangle$. We have divided our discussion in three sections. In Section A, we will discuss the effect of external magnetic field on in-medium behaviour of scalar fields σ, ζ, δ and χ, through which medium dependence of gluon condensates will be evaluated. The in-medium effects on gluon condensates are discussed in Section B. Finally, in Section C, medium modification of J/ψ and η_c meson will be discussed.

4.1 Scalar fields σ, ζ, δ, and χ in hot magnetized nuclear medium

By solving coupled system of non-linear equations (18–23) for σ, ζ, δ, ω, ρ and χ, temperature and density dependence of these fields in the presence of magnetic field is calculated. These equations have the dependence on vector density, ρ_i^v

Table 1 Values of various parameters

$g_{\sigma N}$	$g_{\zeta N}$	$g_{\delta N}$	$g_{\omega N}$	$g_{\rho N}$
10.56	− 0.46	2.48	13.35	5.48
k_0	k_1	k_2	k_3	k_4
2.53	1.35	− 4.77	−2.77	− 0.218
m_π (MeV)	m_K (MeV)	f_π (MeV)	f_K (MeV)	g_4
139	498	93.29	122.14	79.91
σ_0 (MeV)	ζ_0 (MeV)	χ_0 (MeV)	d	ρ_0 (fm^{-3})
− 93.29	− 106.8	409.8	0.064	0.15

and scalar density, ρ_i^s of the nucleons, which further have magnetic field dependency as can be seen from Eqs. (24) to (28). Various parameters used in the present work are listed in Table 1.

In Fig. 1, we show the variation of scalar fields σ, ζ, δ, and χ as a function of temperature T at magnetic field B = $0, 5m_\pi^2$ and $7m_\pi^2$ ($1m_\pi^2 = 2.818 \times 10^{18}$ gauss $= 5.48 \times 10^{-2}$ GeV^2), and nucleon density, $\rho_N = 0$. As can be seen from Fig. 1, at $\rho_N = 0$, the effects of magnetic field are more appreciable above certain high value of temperature. For given temperature, the magnitude of scalar fields σ and ζ and the dilaton fields χ are observed to decrease with increase in magnetic field. Further, in Figs. 2 and 3, we plot these scalar fields individually as a function of temperature T at different magnetic field strength, eB and for finite nucleon density. We show the results at nucleon densities $\rho_N = \rho_0$ (left column) and $4\rho_0$ (right column) and isospin asymmetry, $\eta = 0, 0.3$ and 0.5. Here, e and ρ_0 are the electrostatic unit of charge and nuclear saturation density respectively.

In Fig. 2, we observe that at zero and non-zero values of magnetic field, for finite value of nucleon density ρ_N, the magnitude of scalar fields σ and ζ increases with increase in temperature and then start decreasing after certain value. For example, in symmetric nuclear matter, at $\rho_N = \rho_0$ and $B = 0$, the magnitudes of both σ and ζ fields increase upto temperature $T = 145$ MeV and then start decreasing with further increase in temperature. For finite value of magnetic field B, the magnitude of both scalar fields decreases as compared to $B = 0$, but follows the same functional dependence with respect to temperature. The medium modified values of σ and ζ fields in symmetric nuclear matter are listed in Table 2. The decrease in the magnitude of σ and ζ fields as a function of magnetic field strength will result in decrease in the mass of nucleons (see Eq. 6). Thus, finite magnetic field strength at high temperature will further support the restoration of chiral symmetry and may result in decrease in critical temperature. Moreover, with the rise of temperature, the value of thermal distribution function given in Eqs. (29) and (30) decreases, which results in decrease in the scalar density given by Eqs. (25) and (28). In addition, at $\mu_i^* \neq 0$, *i.e.* for finite density, there are contributions from higher momenta. Thus, the variation of σ and ζ field with respect to temperature reflects the competing effects between the thermal distribution functions and the contributions from higher momenta states [84].

Comparing the behaviour of scalar fields at finite asymmetry of the medium with the symmetric situation, we observe that isospin asymmetric effect on scalar field σ are more appreciable than ζ field. This is related to the fact that the σ field contains non zero isospin quark content, while ζ field quark content is independent of isospin. Therefore, former is more sensitive to non-zero isospin asymmetry parameter, η, than the latter (ζ has little dependence as it is solved along with other scalar fields). For given density and temperature, the decrease in magnitude of scalar fields is observed to be small at $\eta = 0.3$ as compared to $\eta = 0$, as we increase the external magnetic field strength from zero to finite value. However, as we move to $\eta = 0.5$, below T $\cong$ 80 MeV, the magnitude of scalar field σ increases with increase in the magnetic field strength, whereas, above this temperature, the trend is opposite. The reason behind this crossover behaviour is the fact that in pure neutron matter, $\eta = 0.5$, at a particular value of temperature, neutron scalar density, ρ_n^s decrease more slowly as compared to proton scalar density, ρ_p^s. The net effect of ρ_n^s and ρ_p^s results in the above behavior of σ and ζ fields. In the present investigation, the variation of scalar fields and nucleon mass at finite density, temperature and external magnetic field are in accordance with the calculations done under non-linear Walecka model [26]. In this article, authors have studied the properties of stellar matter at finite density, tempearature and uniform magnetic field.

The scalar isovector field δ having contribution due to isospin asymmetry of the medium is plotted in Fig. 3. It is observed that at $\eta = 0$, the δ field is zero for magnetic field $B = 0$, but non-zero for finite magnetic field strength. This is because the δ field is determined by the difference between the scalar densities of neutron and proton. For zero magnetic field, the value of δ field is zero as scalar density of proton is equal to scalar density of neutron (see Eqs. 31, 32). On the other hand, in the presence of magnetic field, due to charged nature of proton, Landau quantization occurs, this leads to the inequality $\rho_p^s \neq \rho_n^s$ (see Eqs. 24, 28), hence non-zero value of the δ is obtained. In the same figure, the dilaton field χ is also plotted, which is introduced in the chiral $SU(3)$ model to preserve broken scale invariance property of QCD at tree level [119]. It is observed that the magnitude of dilaton field χ shows behaviour similar to σ and ζ fields. It first increases up to certain temperature T, then decreases with further increase in temperature. It is observed from the figure that the dilaton field χ varies least as compared to other mesonic fields. Therefore, frozen glueball limit is assumed in many research papers on chiral $SU(3)$ model [9,55]. In the lower density region, the effects of magnetic field on χ

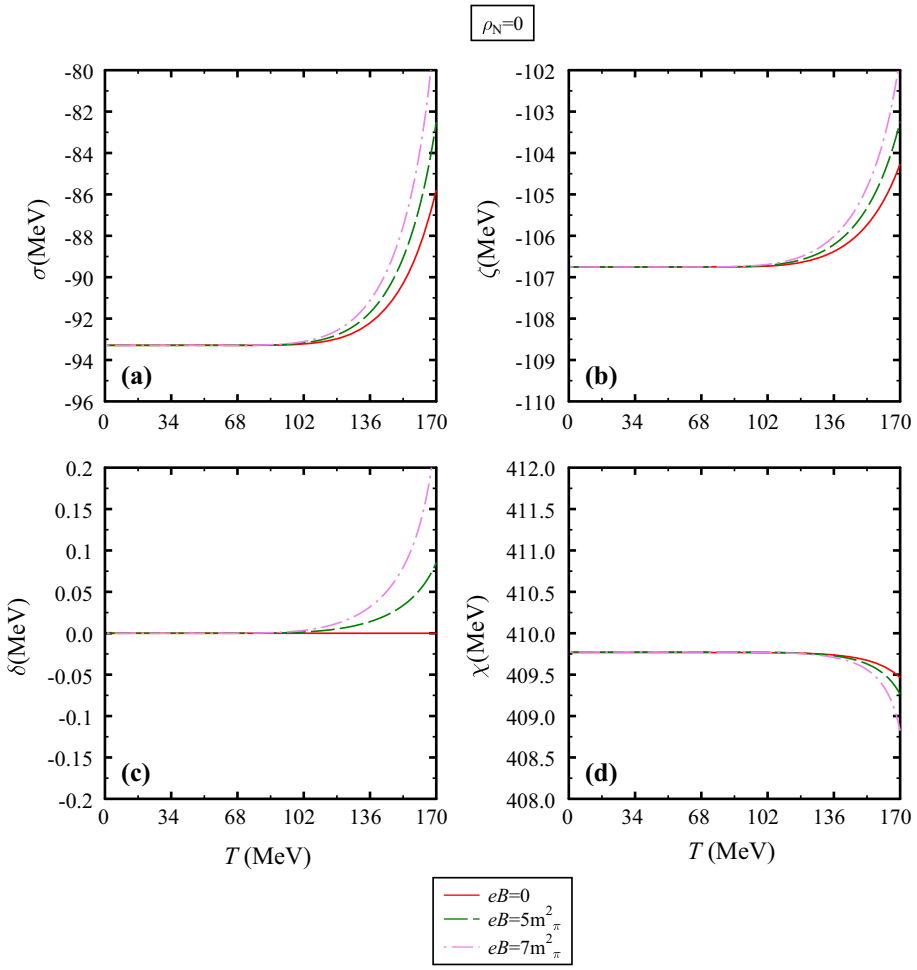

Fig. 1 The scalar fields σ, ζ, δ and χ plotted as a function of temperature T, for different values of magnetic field, B at nucleon density $\rho_N = 0$

field are very less, whereas at high density these become significant.

4.2 In-medium gluon condensate and twist-2 gluon operator

In Fig. 4, we show the variations of scalar gluon condensate G_0 (Eq. 39) as well as the twist-2 gluon operator G_2 (Eq. 40) with temperature for different values of magnetic field, nucleon density and isospin asymmetry parameter. The scalar gluon condensate, G_0 consists of two terms. The first term has the dependence on the fourth power of χ field, whereas the second term contributes the finite quark mass effects from the energy–momentum tensor, which have the σ and ζ field dependence. On the other hand, the twist-2 gluon operator, G_2 has contribution of three terms, which further have the dependency on scalar fields. Although, the condensates G_0 and G_2 depends upon all scalar fields (see Eqs. 39, 40), but the observed behaviour resembles χ field due to its fourth power dependence. For better understanding of condensate's behaviour, the different terms of G_0 and G_2 are plotted in Fig. 5 considering finite quark mass term contribution to scalar gluon condensates, in symmetric nuclear medium, at temperature $T = 0$ (100) MeV, the values of G_0, in units of 10^{-2} GeV^4, are observed to be 1.842 (1.871), 1.809 (1.838) and 1.764 (1.800) at $eB = 0, 5m_\pi^2$ and $7m_\pi^2$, respectively. However, in massless quark limit (Eq. 38) these values changes to 2.177 (2.210), 2.139 (2.172) and 2.089 (2.130). In addition, the tensorial gluon operator, G_2 varies very less in high density as compared with low density as a function of temperature. This behaviour reflects the competing effects between the second and third term of Eq. (40) plotted in Fig. 5. The crossover behaviour of condensates in highly asymmetric nuclear medium reflects the χ field, which is solved along with the σ, ζ and δ fields. For example, in symmetric nuclear matter, at $\rho_N = 4\rho_0$ and temperature $T = 0$ (100) MeV, the values of χ field are observed to be 402.2 (403.5), 400.4 (402) and 398.1 (400) MeV for $eB = 0, 5m_\pi^2$ and $7m_\pi^2$ respectively and for $\eta = 0.5$, these values changes to 403.2 (404.1), 403.8 (403.9) and 404.3 (403.3). In vacuum, the twist-2 gluon operator vanishes due to the Lorentz symmetry. But in the current investigation, the presence of finite density, temperature and magnetic field breaks the Lorentz symmetry, hence non-vanishing value of G_2 is obtained [77,117]. The observed

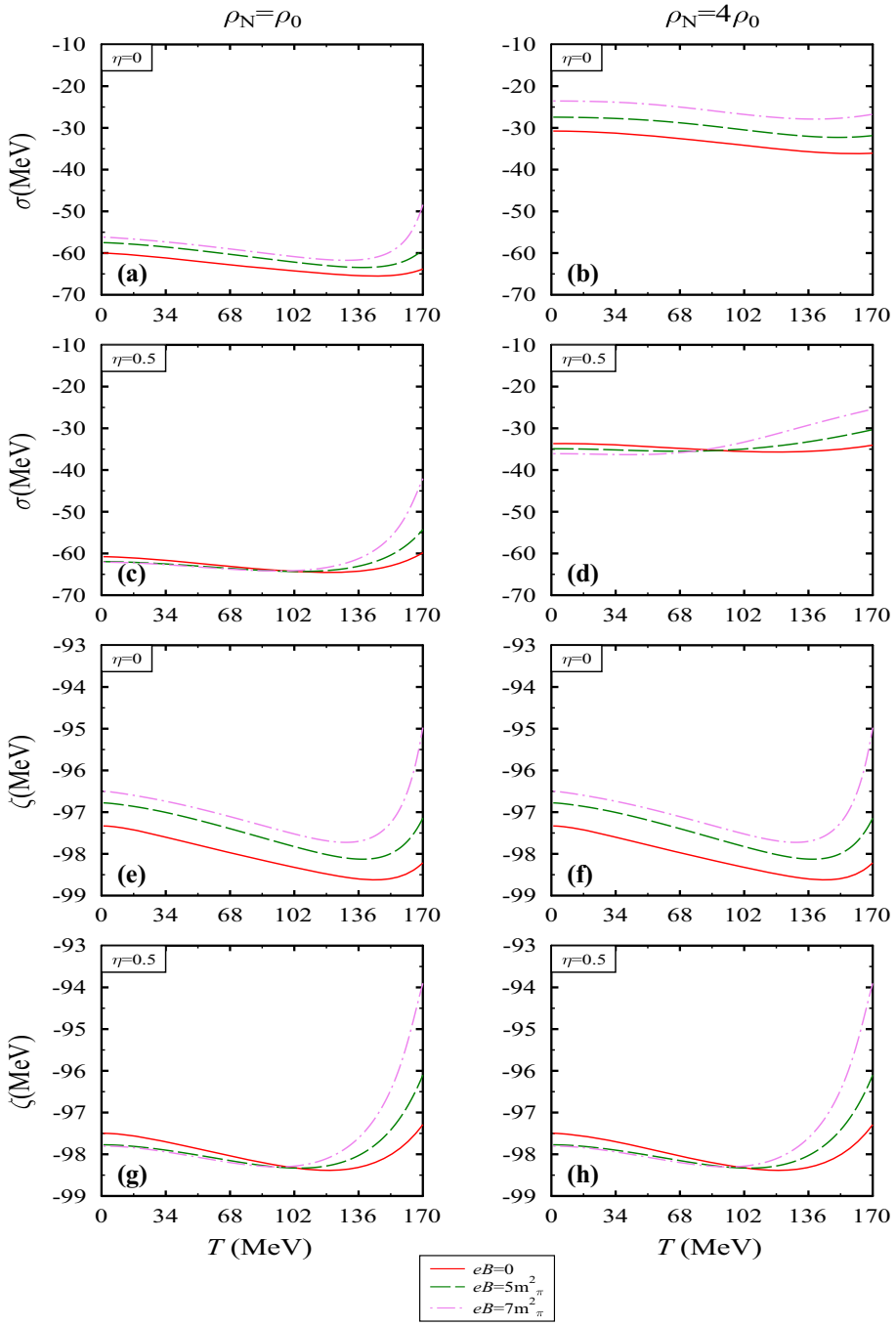

Fig. 2 The scalar fields σ and ζ plotted as a function of temperature T, for different values of magnetic field, B, nucleon density ρ_N and isospin asymmetry parameter, η

behaviour of G_0 and G_2 as a function of temperature at zero magnetic field and nucleon density is consistent with the condensates behaviour observed in Ref. [117].

4.3 In-medium masses of J/ψ and η_c

In this section, we calculate the in-medium mass shift of J/ψ and η_c mesons, using medium modified scalar and tensorial gluon condensate, by applying QCD sum rules. In this application, we use the moment in the range $5 \leq n \leq 9$ and $7 \leq n \leq 10$ for J/ψ and η_c mesons respectively to get the mass in stable region. We have used $\xi = 1$ and corresponding running charm quark mass, $m_c = 1228.52$ MeV as well as parameter, $\alpha_s = 0.2636$. In Eqs. (47) and (49), we obtain the value of ϕ_b and ϕ_c using medium modified gluon condensates within the chiral $SU(3)$ model and are used to calculate moment M_n^J, and hence the in-medium charmonium mass m_C^*, under QCD sum rules. The obtained values of ϕ_b and ϕ_c are tabulated in the Table 3. At $T = 0$ and $\rho_N = \rho_0$, the above values of ϕ_b can be compared with the

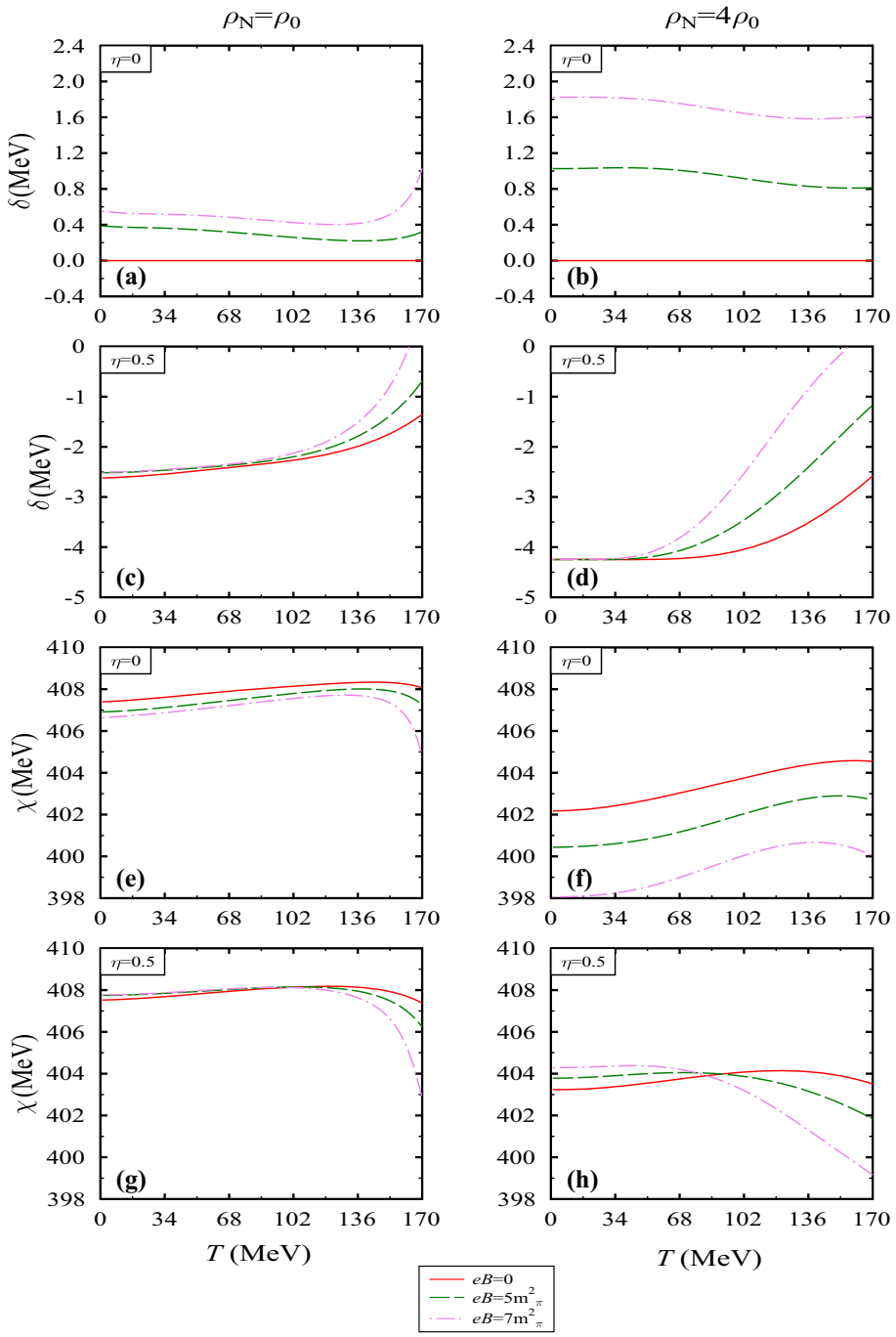

Fig. 3 The scalar fields δ and χ plotted as a function of temperature T, for different values of magnetic field, B, nucleon density ρ_N and isospin asymmetry parameter, η

Table 2 In the above table, we tabulate the in-medium values of scalar fields σ and ζ (in MeV) in symmetric nuclear matter for different values of magnetic field, eB, nucleon density ρ_N and temperature T (in MeV)

eB (m_π^2)	σ				ζ			
	$T=0$		$T=100$		$T=0$		$T=100$	
	ρ_0	$4\rho_0$	ρ_0	$4\rho_0$	ρ_0	$4\rho_0$	ρ_0	$4\rho_0$
0	− 60.02	− 30.76	− 64.19	− 34.10	− 97.33	− 92.84	− 98.30	−93.20
5	− 57.51	− 27.43	− 62.07	−30.37	− 96.78	−92.54	− 97.80	− 92.80
7	− 56.19	− 23.55	−60.76	− 26.67	− 96.50	−92.29	− 97.50	− 92.48

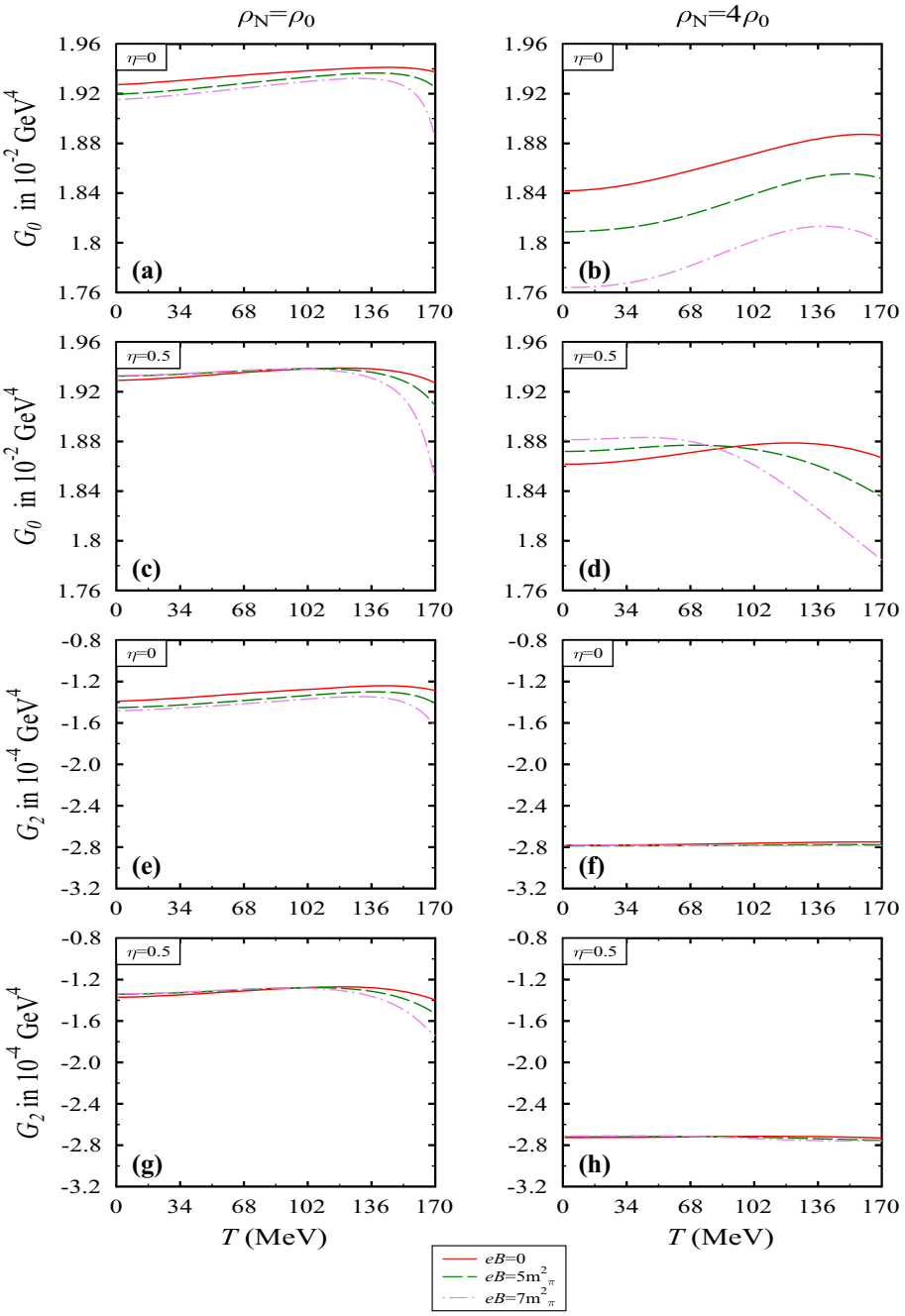

Fig. 4 The scalar gluon condensate G_0 and tensorial gluon condensate G_2 (describing the trace and non-trace part of energy momentum tensor respectively) plotted as a function of temperature T, for different values of magnetic field, B, nucleon density ρ_N and isospin asymmetry parameter, η

Table 3 In the above table, we tabulate the values of ϕ_b and ϕ_c under the effect of magnetic field, temperature (in MeV) and density

eB (m_π^2)	ϕ_b in unit of 10^{-3}				ϕ_c in unit of 10^{-5}			
	$T=0$		$T=100$		$T=0$		$T=100$	
	ρ_0	$4\rho_0$	ρ_0	$4\rho_0$	ρ_0	$4\rho_0$	ρ_0	$4\rho_0$
0	2.30	2.20	2.29	2.19	− 5.01	− 0.1	− 4.61	− 0.1
5	2.29	2.18	2.28	2.15	− 5.24	− 0.1	− 4.82	− 0.1
7	2.29	2.14	2.27	2.09	− 5.35	− 0.1	− 4.95	− 0.1

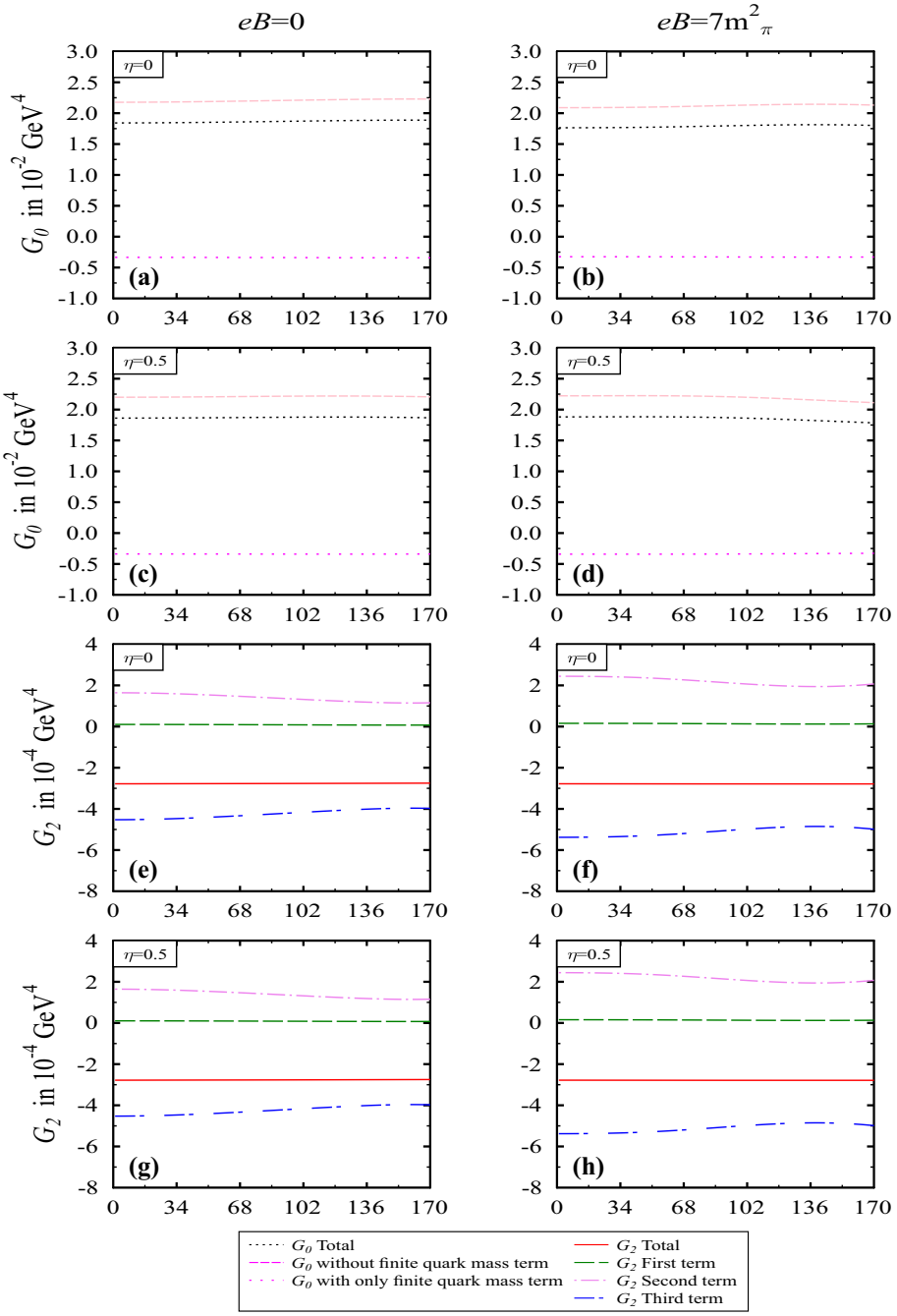

Fig. 5 The individual terms of scalar gluon condensate G_0 and tensorial gluon condensate G_2 plotted as a function of temperature T, for different values of magnetic field, B, and isospin asymmetry parameter, η at nucleon density $\rho_N = 4\rho_0$

values 1.7×10^{-3} and 1.6×10^{-3} at vacuum and nuclear saturation density respectively in Ref. [77]. We plot in-medium mass of J/ψ and η_c in Figs. 6, 7, and 8 for isospin asymmetry $\eta = 0, 0.3$ and 0.5 respectively. We show the results for J/ψ and η_c at $T = 0$,100 MeV and $\rho_N = \rho_0$,$4\rho_0$ and for magnetic field $eB = 0, 5m_\pi^2$ and $7m_\pi^2$. In each subplot the results are compared with vacuum situation, *i.e.* $\rho_N = B = T = 0$. In Table 4, we summarize the values of mass-shift of J/ψ and η_c at $eB = 5m_\pi^2$ and $7m_\pi^2$ from the values at $B = 0$.

From Fig. 6 we observe that, for given density and temperature, the finite magnetic field causes more decrease in masses of J/ψ and η_c mesons. However, we observe less decrease in mass of J/ψ and η_c, as we move from $T = 0$ to $T = 100$ MeV. The negative mass-shift due to magnetic field is more in high density regime. For example, at $\rho_N = \rho_0$, $\eta = 0$ and $T = 0$, the mass-shift of J/ψ and η_c is -3.39 (-3.68) and -4.63 (-5.07) MeV for $eB = 5m_\pi^2$ ($7m_\pi^2$) with respect to vacuum mass respectively, whereas at $4\rho_0$, the mass-shift modifies to -11.63 (-14.68) and -11.97 (-12.96) MeV . This is due to the fact that at high density the values of gluon condensates decrease more with the increase of magnetic field, which further modify ϕ_b

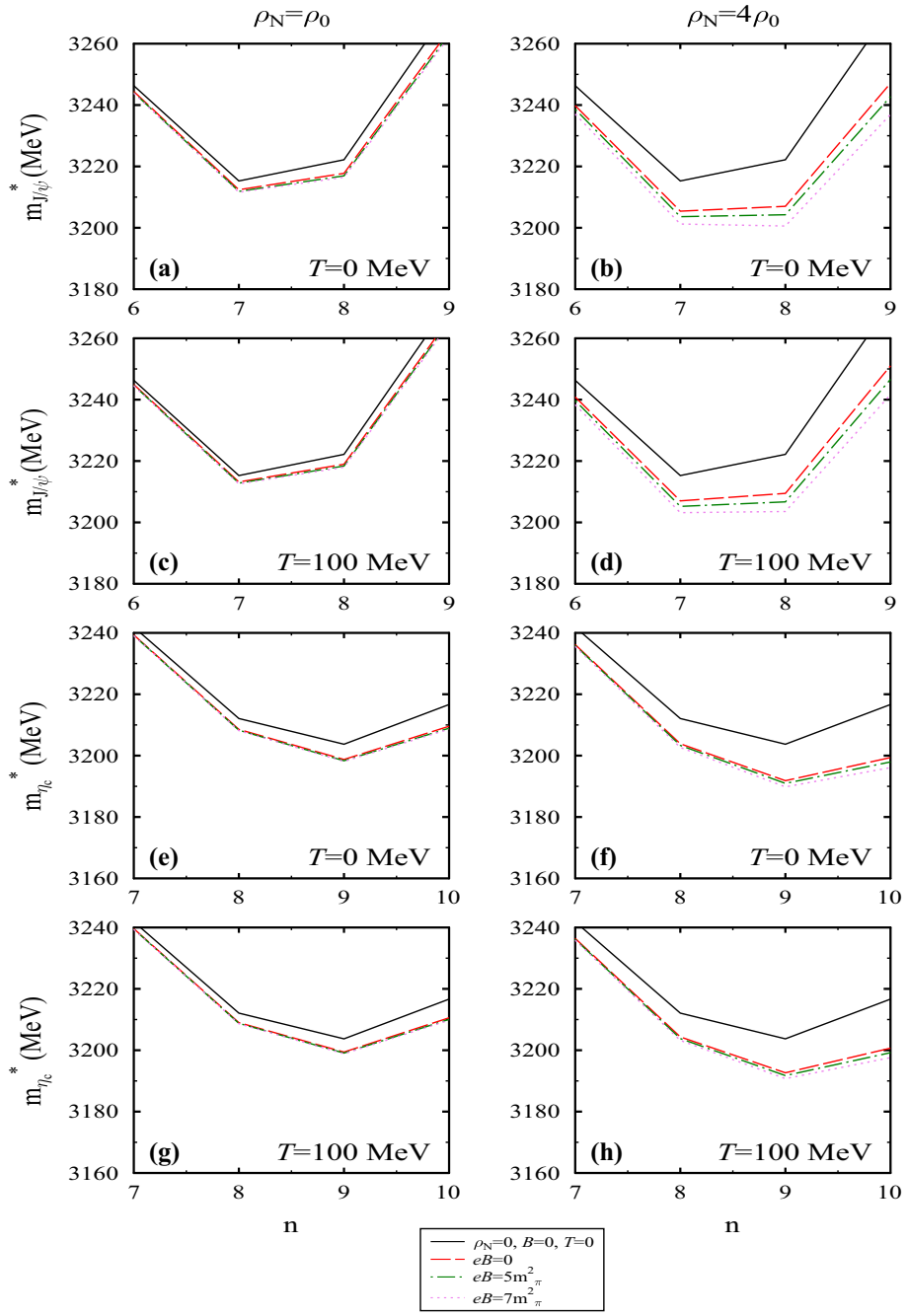

Fig. 6 The in-medium mass of J/ψ and η_c meson plotted as a function of n for symmetric nuclear matter at different values of temperature, magnetic field and density

and ϕ_c and finally J/ψ and η_c. In Ref. [104], using chiral $SU(3)$ model with QCD second order stark effect, authors have reported the J/ψ mass-shift in finite magnetic field with respect to vacuum at zero temperature. In this article, it was observed that, at $\eta = 0$, and $\rho_N = \rho_0$, the mass-shift is $-$ 8.16 MeV for both $eB = 4m_\pi^2$ and $8m_\pi^2$ with respect to vacuum mass . In Ref. [10], using QCD sum rules, the mass shift of J/ψ and η_c is calculated in strong magnetic field at zero density and temperature and observed to decrease with increase in eB.

For given density and temperature, as we increase the isospin asymmetry of the medium from $\eta = 0$ to 0.5, less negative mass-shift is observed at finite magnetic field from zero magnetic field situation. In other words, finite isospin asymmetry of the medium causes an increase in the mass of charmonium states. The observed behaviour is again due to such dependence of gluon condensates on the isospin asymmetry of nuclear medium. At $\eta = 0.5$, the mass-shift can be compared with value, $-$ 7.86 MeV at $eB = 8m_\pi^2$ obtained in Ref. [104]. In the present investigation, at $\eta = 0.5$, positive mass-shift is observed in low temperature regime and is

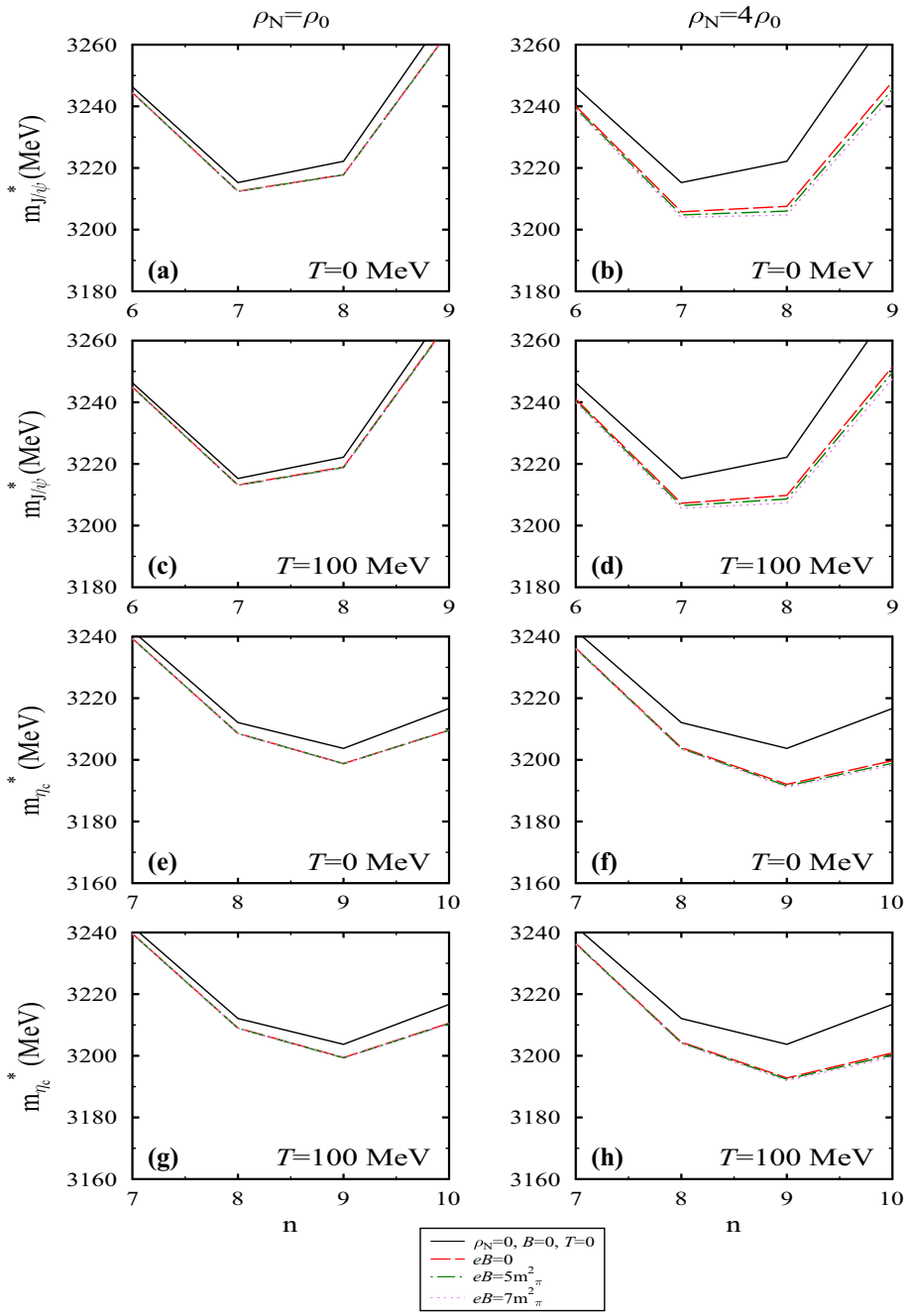

Fig. 7 The in-medium mass of J/ψ and η_c meson plotted as a function of n for asymmetric nuclear matter, $\eta = 0.3$ at different values of temperature, magnetic field and density

given in Table 4. The above variation is due to the observed crossover of scalar densities of nucleons and scalar fields σ and ζ as shown in Fig. 2.

In Fig. 6, when there is no external magnetic field and isospin asymmetry, it is observed that the mass-shift of J/ψ and η_c mesons with respect to vacuum mass are $-$ 2.86 ($-$ 2.08) MeV and $-$ 4.96 ($-$ 4.30) MeV at $T = 0$ (100) MeV and $\rho_N = \rho_0$. These values of mass-shift can also be compared with the mass-shift of J/ψ and η_c mesons, having $-$ 7 and $-$ 5 MeV, respectively, investigated in QCD sum rules under linear density approximation [77].

In the next section, we will now summarize our present work.

5 Summary

In this article, we have studied the effects of strong magnetic field on the in-medium mass of lowest charmonia, namely J/ψ and η_c, in hot and dense isospin asymmetric nuclear matter using chiral $SU(3)$ model along with QCD sum rules. In effective chiral model, nucleons properties are modified

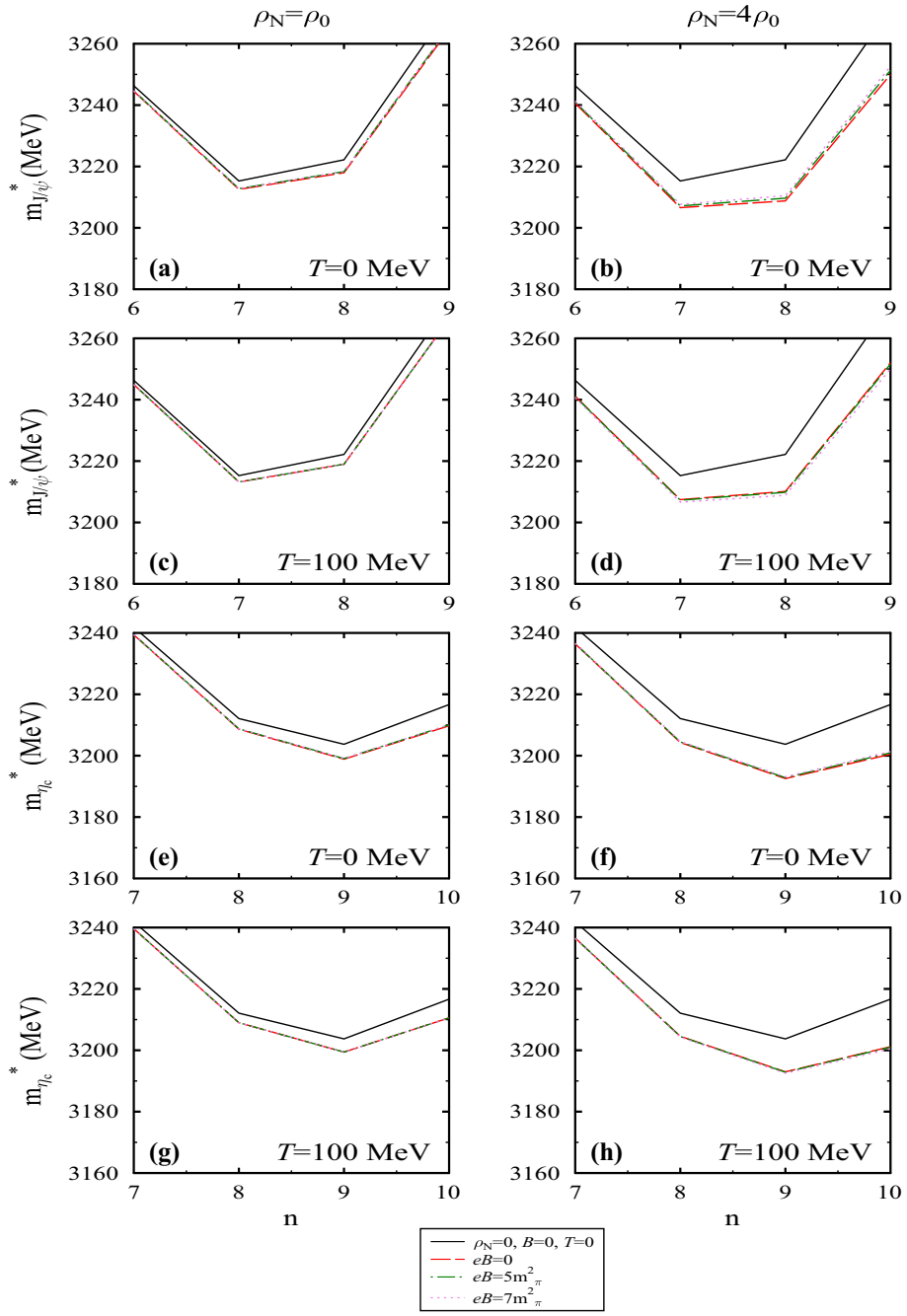

Fig. 8 The in-medium mass of J/ψ and η_c meson plotted as a function of n for asymmetric nuclear matter, $\eta = 0.5$ at different values of temperature, magnetic field and density

Table 4 In the above table, we tabulate the effect of magnetic field on the mass-shifts of J/ψ and η_c mesons. Here, $\Delta m_{B_{50}}$ represents mass-shift between $eB = 5m_\pi^2$ and B = 0 (similar for $\Delta m_{B_{70}}$). In addition, temperature T and ρ_N are given in units MeV and fm^{-3} respectively

	Δm_B	$\eta = 0$				$\eta = 0.3$				$\eta = 0.5$			
		$T = 0$		$T = 100$		$T = 0$		$T = 100$		$T = 0$		$T = 100$	
		ρ_0	$4\rho_0$	ρ_0	$4\rho_0$	ρ_0	$4\rho_0$	ρ_0	$4\rho_0$	ρ_0	$4\rho_0$	ρ_0	$4\rho_0$
J/ψ	$\Delta m_{B_{50}}$	− 0.54	−1.79	− 0.39	−1.80	− 0.03	−1.01	− 0.12	− 0.77	0.24	0.57	− 0.01	− 0.18
	$\Delta m_{B_{70}}$	− 0.84	−4.84	− 0.65	−3.85	− 0.11	−1.83	− 0.07	−1.63	0.27	1.10	− 0.02	− 0.83
η_c	$\Delta m_{B_{50}}$	− 0.44	− 0.88	− 0.36	− 0.92	− 0.04	− 0.52	− 0.11	− 0.41	0.20	0.29	− 0.01	− 0.11
	$\Delta m_{B_{70}}$	− 0.68	−2.02	− 0.59	−1.92	− 0.10	− 0.92	− 0.18	− 0.85	0.23	0.57	− 0.01	− 0.46

through σ, ζ, δ, and χ fields resulting in the in-medium modifications of gluon condensates and masses of J/ψ and η_c. This interaction also accounts for scalar and number density of nucleons under the effect of magnetic field. For proton, since it has non-zero charge, we have contributions from the Landau levels hence it has strong influence, whereas for neutrons (zero charge) there are no Landau level contributions. Mainly, the in-medium modifications of J/ψ and η_c owes to the change in scalar gluon condensate and twist-2 gluon operator, which is obtained from the medium modification of scalar fields σ, ζ, δ, and χ. These fields in strongly magnetized hot and dense isospin asymmetric (introduced by the δ and ρ fields) nuclear matter is obtained by solving the coupled equations of motions (Eqs. 18–23). We have observed that the effective mass of J/ψ and η_c decrease with the increase in magnetic field except in the case of low-temperature regime of high isospin asymmetry, where increase in effective mass is observed due to the crossover behaviour of scalar fields and scalar densities of protons and neutrons. The mass modifications of these mesons are observed to be appreciable in high density and symmetric nuclear matter. It is also observed that the masses of vector meson, J/ψ and pseudoscalar meson, η_c increase as we move towards high temperature. The observed mass-shift may be used to study the decay of charmonia [121] in the presence of magnetic field. The present work will shed light on non-perturbative effects of magnetic field on the properties of mesons and hadrons, which may help to understand the experimental observables such as decay width [120,121] and cross-section [122], in asymmetric non-central heavy ion collision experiments.

Acknowledgements One of the author, Rajesh Kumar sincerely acknowledge the support towards this work from Ministry of Science and Human Resources Development (MHRD), Government of India via Institute fellowship under National Institute of Technology Jalandhar.

Data Availability Statement This manuscript has no associated data or the data will not be deposited. [Authors' comment: Work involve the theoretical calculations and no other data is used which could be deposited.]

Funded by SCOAP[3].

References

1. D.E. Kharzeev et al., Nucl. Phys. A **803**, 227 (2008)
2. K. Fukushima et al., Phys. Rev. D **78**, 074033 (2008)
3. V.V. Skovov et al., Int. J. Mod. Phys. A **24**, 5925 (2009)
4. K. Tuchin, Phys. Rev. C **83**, 017901 (2011)
5. K. Tuchin, Phys. Rev. C **82**, 034904 (2011)
6. K. Tuchin, Phys. Rev. C **88**, 024911 (2013)
7. K. Marasinghe, K. Tuchin, Phys. Rev. C **84**, 044908 (2011)
8. A. Das et al., Phys. Rev. C **96**, 034902 (2017)
9. R.P. Sushruth et al., Phys. Rev. C **97**, 065208 (2018)
10. S. Cho et al., Phys. Rev. D **91**, 045025 (2015)
11. D. Kharzeev et al., *Strongly Interacting Matter in Magnetic Fields* (Springer, Berlin, 2013)
12. A. Vilenkin, Phys. Rev. D **22**, 3080 (1980)
13. Y. Burnier et al., Phys. Rev. Lett. **107**, 052303 (2011)
14. G.S. Bali et al., J. High Energy Phys. **2013**, 130 (2013)
15. S. Ozaki, Phys. Rev. D **89**, 054022 (2014)
16. S. Schramm et al., Mod. Phys. Lett. A **07**, 973 (1992)
17. D.K. Hong et al., Phys. Rev. D **54**, 7879 (1996)
18. D.K. Hong, Phys. Rev. D **57**, 3759 (1998)
19. G.W. Semenoff et al., Phys. Rev. D **60**, 105024 (1999)
20. G.S. Bali et al., J. High Energy Phys. **2012**, 44 (2012)
21. C.N. Leung et al., Phys. Rev. D **54**, 4181 (1996)
22. S. Cho et al., Phys. Rev. Lett. **113**, 172301 (2014)
23. P. Gubler et al., Phys. Rev. D **93**, 054026 (2016)
24. J. Alford, M. Strickland, Phys. Rev. D **88**, 105017 (2013)
25. S. Gupta, Phys. Lett. B **597**, 57 (2004)
26. A. Rabhi et al., Phys. Rev. C **84**, 035803 (2011)
27. R.C. Duncan, C. Tompson, Astrophys. J. **392**, L9 (1992)
28. C. Kouvellioton, Nature **393**, 235 (1998)
29. S. Mareghetti, L. Stella, Astrophys. J. **442**, L17 (1995)
30. S.L. Shapiro, S.A. Teukolsky, *Black Holes, White Dwarfs and Neutron Stars* (Wiley, New York, 1983)
31. L. Ferrario, D. Wickrammasinghe, MNRAS **367**, 1323 (2006)
32. A. Iwazaki, Phys. Rev. D **72**, 114003 (2005)
33. A. Broderick et al., Astrophys. J. **537**, 351 (2000)
34. C.Y. Cardall et al., Astrophys. J. **554**, 322 (2001)
35. D. Bandyopadhyay et al., Phys. Rev. Lett. **79**, 2176 (1997)
36. G.-J. Mao et al., Chin. J. Astron. Astrophys. **3**, 359 (2003)
37. A. Rabhi, C. Providencia, J. Phys. G **35**, 125201 (2008)
38. D.T. Son, A.R. Zhitnitsky, Phys. Rev. D **70**, 074018 (2004)
39. D.T. Son, Phys. Rev. B **75**, 235423 (2007)
40. D. Kharzeev, A. Zhitnitsky, Nucl. Phys. A **797**, 67 (2007)
41. R. Rapp, H. van Hees. arXiv:0803.0901v2 [hep-ph] (2008)
42. V. Gusynin et al., Phys. Rev. Lett. **73**, 3499 (1994)
43. K.G. Wilson, Phys. Rev. D **10**, 2445 (1974)
44. B.B. Brandt et al., Phys. Rev. D **97**, 054514 (2018)
45. J.B. Kogut, D.K. Sinclair, Phys. Rev. D **66**, 014508 (2002)
46. J.B. Kogut, D.K. Sinclair, Phys. Rev. D **70**, 094501 (2004)
47. S. Muroya, A. Nakamura, C. Nonaka et al., Prog. Theor. Phys. **110**, 615 (2003)
48. J.C.R. Bloch, T. Wettig, J. High Energy Phys. **0903**, 100 (2009)
49. K. Fukushima, Y. Hidaka, Phys. Rev. D **75**, 036002 (2007)
50. J.D. Walecka, Ann. Phys. **83**, 491 (1974)
51. Y. Nambu, G. Jona-Lasinio, Phys. Rev. **122**, 345 (1961)
52. K. Fukushima, Phys. Lett. B **591**, 277 (2004)
53. K. Kashiwa et al., Phys. Lett. B **662**, 26 (2008)
54. S.K. Ghosh et al., Phys. Rev. D **91**, 054005 (2015)
55. P. Papazoglou et al., Phys. Rev. C **59**, 411 (1999)
56. A. Mishra et al., Phys. Rev. C **69**, 015202 (2004)
57. A. Mishra et al., Eur. Phys. J. A **41**, 205 (2009)
58. A. Kumar, A. Mishra, Phys. Rev. C **82**, 045207 (2010)
59. A. Kumar, A. Mishra, Eur. Phys. J. A **47**, 164 (2011)
60. L. Tolós et al., Phys. Rev. C **763**, 025203 (2004)
61. L. Tolós et al., Phys. Lett. B **635**, 85 (2006)
62. L. Tolós et al., Phys. Rev. C **77**, 015207 (2008)
63. J. Hofmann, M.F.M. Lutz, Nucl. Phys. A **763**, 90 (2005)
64. P.A.M. Guichon, Phys. Lett. B **200**, 235 (1988)
65. S.W. Hong, B.K. Jennings, Phys. Rev. C **64**, 038203 (2001)
66. K. Tsushima et al., Phys. Rev. C **59**, 2824 (1999)
67. A. Sibirtsev et al., Eur. Phys. J. A **6**, 351 (1999)
68. K. Saito, A.W. Thomas, Phys. Lett. B **327**, 9 (1994)

69. P.K. Panda et al., Phys. Rev. C **56**, 3134 (1997)
70. B.J. Schaefer et al., Phys. Rev. D **81**, 074013 (2010)
71. S. Chatterjee, K.A. Mohan, Phys. Rev. D **85**, 074018 (2012)
72. L.J. Reinders et al., Nucl. Phys. B **186**, 109 (1981)
73. A. Hayashigaki, Phys. Lett. B **487**, 96 (2000)
74. T. Hilger et al., Phys. Rev. C **79**, 025202 (2009)
75. L.J. Reinders et al., Phys. Rep. **127**, 1 (1985)
76. F. Klingl et al., Nucl. Phys. A **624**, 527 (1997)
77. F. Klingl et al., Phys. Rev. Lett. **82**, 3396 (1999)
78. K. Morita, S.H. Lee, Phys. Rev. C **85**, 044917 (2012)
79. S. Kim, S.H. Lee, Nucl. Phys. A **679**, 517 (2001)
80. K. Suzuki et al., Nucl. Phys. A **897**, 28 (2013)
81. A. Mishra, D. Pathak, Phys. Rev. C **90**, 025201 (2014)
82. M.A. Shifman et al., Phys. Lett. B **77**, (1978)
83. R. Chhabra, A. Kumar, Eur. Phys. J. A **53**, 105 (2017)
84. A. Mishra et al., Phys. Rev. C **69**, 024903 (2004)
85. D. Zschiesche et al., Phys. Rev. C **70**, 045202 (2004)
86. T.K. Herbst et al., Phys. Lett. B **731**, 248 (2014)
87. M. Drews et al., Phys. Rev. D **88**, 096011 (2013)
88. V. Skokov et al., Phys. Rev. C **82**, 015206 (2010)
89. B.J. Schaefer et al., Phys. Rev. D **76**, 074023 (2007)
90. T.K. Herbst et al., Phys. Lett. B **696**, 58 (2011)
91. E. Nakano et al., Phys. Lett. B **682**, 401 (2010)
92. T. Matsui, H. Satz, Phys. Lett. B **178**, 416 (1986)
93. (NA50 Collaboration) B. Alessandro et al., Eur. Phys. J. C **39**, 335 (2005)
94. (NA60 Collaboration) Arnaldi et al., Phys. Rev. Lett. **99**, 132302 (2007)
95. (PHENIX Collaboration) A. Adare et al., Phys. Rev. Lett. **98**, 249902 (2007)
96. E.G. Ferreiro, Phys. Lett. B **731**, 57 (2014)
97. L. Grandchamp, R. Rapp, Nucl. Phys. A **709**, 415 (2002)
98. A. Andronic et al., Phys. Lett. B **571**, 36 (2003)
99. S.H. Lee, C.M. Ko, Phys. Rev. C **67**, 038202 (2003)
100. C.A. Dominguez et al., Phys. Rev. D **81**, 014007 (2010)
101. A. Mocsy, J. Phys. G Nucl. Part. Phys. **34**, S745 (2007)
102. M. Asakawa, T. Hatsuda, Phys. Rev. Lett. **92**, 012001 (2004)
103. Y.-H. Song et al., Phys. Rev. C **79**, 014907 (2009)
104. C.S. Amal Jahan, et al. arXiv:1803.04322v1 [nucl-th] (2018)
105. S. Ghosh et al., Phys. Rev. D **94**, 094043 (2016)
106. C.S. Machado et al., Phys. Rev. D **89**, 074027 (2014)
107. G. Krein et al., Phys. Lett. B **697**, 136 (2011)
108. S.J. Brodsky, I. Schmidt, Phys. Rev. Lett. **64**, 1011 (1990)
109. S. Weinberg, Phys. Rev. **166**, 1568 (1968)
110. S. Coleman et al., Phys. Rev. **177**, 2239 (1969)
111. W.A. Bardeen, B.W. Lee, Phys. Rev. **177**, 2389 (1969)
112. D. Zschiesche, Description of Hot, Dense, and Strange Hadronic Matter in a Chiral $SU(3)_L \times SU(3)_R$ σ-Model, Thesis (1997)
113. M. Strickland et al., Phys. Rev. D **86**, 125032 (2012)
114. I. Ternov et al., Moscow Univ. Phys. Bull. (English Transl.) **21**, 21 (1966)
115. A.E. Broderick et al., Phys. Lett. B **531**, 167 (2002)
116. S.H. Lee, K. Morita, Pramana **72**, 97 (2009)
117. K. Morita, S.H. Lee, Phys. Rev. C **77**, 064904 (2008)
118. K.G. Wilson, Phys. Rev. **179**, 1499 (1969)
119. J. Schechter, Phys. Rev. D **21**, 3393 (1980)
120. Y.S. Golubeva et al., Eur. Phys. J. A **17**, 275 (2003)
121. B. Friman et al., Phys. Lett. B **548**, 153 (2002)
122. (CMS Collaboration) V. Khachatryan et al., Phys. Lett. B **772**, 489 (2017)